Research Article

Shahina Anwarul*, Tanupriya Choudhury*, and Susheela Dahiya

A novel hybrid ensemble convolutional neural network for face recognition by optimizing hyperparameters

https://doi.org/10.1515/nleng-2022-0290
received February 21, 2023; accepted April 4, 2023

Abstract: A fully fledged face recognition system consists of face detection, face alignment, and face recognition. Facial recognition has been challenging due to various unconstrained factors such as pose variation, illumination, aging, partial occlusion, low resolution, *etc*. The traditional approaches to face recognition have some limitations in an unconstrained environment. Therefore, the task of face recognition is improved using various deep learning architectures. Though the contemporary deep learning techniques for face recognition systems improved overall efficiency, a resilient and efficacious system is still required. Therefore, we proposed a hybrid ensemble convolutional neural network (HE-CNN) framework using ensemble transfer learning from the modified pre-trained models for face recognition. The concept of progressive training is used for training the model that significantly enhanced the recognition accuracy. The proposed modifications in the classification layers and training process generated best-in-class results and improved the recognition accuracy. Further, the suggested model is evaluated using a self-created criminal dataset to demonstrate the use of facial recognition in real-time. The suggested HE-CNN model obtained an accuracy of 99.35, 91.58, and 95% on labeled faces in the wild (LFW), cross pose LFW, and self-created datasets, respectively.

Keywords: ensemble learning, face detection, face recognition, hyperparameters tuning, transfer learning

1 Introduction

The need for biometric security solutions is increasing day by day to protect against theft, fraud, *etc*. Face recognition is a key component of biometric security systems [1,2], and it has become an effective tool for several uses, including disease diagnosis, forensic investigations, secure transactions, age estimation, finding the missing, identifying people for e-passports, mask detection, and others [3]. The analysis and comparison of essential facial features and expressions make face identification. It is a technology that aims to make our world more intelligent and safer. It can be used for verification as well as recognition of an individual. The basic steps to implement the pipeline of any face recognition system are shown in Figure 1.

In the face detection and recognition field, a more substantial study has been undertaken [4]. The field is separated into two categories: conventional and deep learning-based. There are various constraints present with traditional approaches, such as they do not provide efficient recognition results in the presence of unconstrained factors. On the other hand, extensive efforts have been made in deep learning to improve facial recognition and address the limitations of conventional methods. However, the deep learning methods' reliance on large amounts of data and extensive computational resources are drawbacks. This limitation of deep learning can be overcome by using deep transfer learning [5]. The practice of transfer learning involves utilizing a previously trained model as a foundation for a new task within the domain of machine learning. In transfer learning, the knowledge

* **Corresponding author: Shahina Anwarul,** School of Computer Science, University of Petroleum and Energy Studies (UPES), Bidholi, Dehradun, 248007, Uttarakhand, India, e-mail: shahinaanwarul@gmail.com, sanwarul@ddn.upes.ac.in
* **Corresponding author: Tanupriya Choudhury,** School of Computer Science, University of Petroleum and Energy Studies (UPES), Bidholi, Dehradun, 248007, Uttarakhand, India; CSE Department, Graphic Era Hill University, Dehradun, 248002, Uttarakhand, India; The AI University, Cutbank, Montana, 59427, United States, e-mail: tanupriya@ddn.upes.ac.in, tanupriyachoudhury@gehu.ac.in, tanupriya1986@gmail.com
Susheela Dahiya: Department of Computer Science and Engineering, Graphic Era Hill University, Dehradun, 248002, Uttarakhand, India
ORCID: Shahina Anwarul 0000-0002-5536-2901; Tanupriya Choudhury 0000-0002-9826-2759; Susheela Dahiya 0000-0003-0318-8427

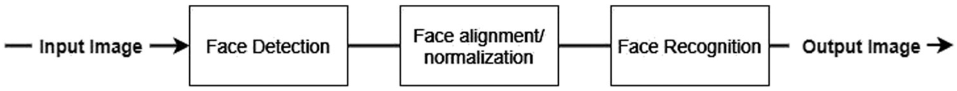

Figure 1: The process pipeline of the face recognition system.

gained by the model during the initial training is leveraged to improve the learning and performance of the model on a new, related task. The application of transfer learning can prove particularly beneficial when either the new task has scarce annotated data or the data distribution of the new task differs from that of the original task. Furthermore, by reusing the pre-trained model, transfer learning can save time and computational resources while improving the accuracy and generalization of the model [6]. The recent surge of machine learning and deep learning used in various applications drives the automation of all tasks [7–9]. Convolutional neural networks (CNNs) play a significant role in implementing deep learning-based approaches. Deep learning CNNs can automatically detect higher-level features from data instead of manually selecting the features [10]. A group of small CNNs was trained to learn DeepID [11], which reached a recognition accuracy of 97.45%. The areas of the face image, such as the eyes, nose, and mouth, are sent to each CNN independently to train it, and then the learned features are combined to produce a potential model. The other deep learning-based algorithms for face recognition, like deep face recognition [12], achieved 98.95% recognition accuracy in the labeled faces in the wild (LFW) [13] and 97.3% recognition accuracy in the YouTube faces (YTF) [14] dataset. In the study of Wen *et al.* [15], a robust CNN was trained using a combination of softmax loss and center loss to extract deep features that enhance inter-class dispersion and intra-class compactness, crucial factors for accurate face recognition. The resulting model achieved impressive recognition accuracy rates of 99.28% on the LFW dataset and 94.9% on YTF.

The shortcomings observed in previous deep learning-based approaches for facial recognition consist of the need for copious amounts of data and advanced computational infrastructure, thereby highlighting the necessity for a resilient recognition system. Furthermore, the large volume of annotated face datasets for face recognition in video surveillance tasks is challenging to acquire due to the privacy concern of the individual. Thus, the proposed approach introduced a novel hybrid ensemble convolutional neural network (HE-CNN) by utilizing deep ensemble learning [16] from the rectified pre-trained models for face recognition. Tang *et al.* [17] proposed an ensemble model of CNN and local binary pattern (LBP). LBP operator is used to extract texture-related features from the face. Ten CNNs with five distinct network structures are employed to extract features further for training, optimizing the network parameters, and obtaining a classification result when the layer is fully connected (FC). The outcome of face recognition is generated using the parallel ensemble learning approach, which involves a majority vote. Alhanaee *et al.* [18] used the concept of deep transfer learning concept in a face recognition-based smart attendance system. They have used the knowledge of pre-trained models to calculate the recognition accuracy on their dataset. The limitation of these state-of-the-art approaches (SOTA) is that they employed the fundamental datasets, in which only a small number of uncontrolled factors are present to evaluate their model. We utilized the concepts of transfer learning and ensemble learning in the proposed model, which helps to overcome the problems mentioned in the existing SOTA. Ensemble learning enhances recognition accuracy by averaging the weights of different deep-learning models. Furthermore, it benefits from deep and ensemble learning for the final model's higher generalization performance [19]. In the suggested method, progressive training [20] is employed to improve the recognition accuracy of the model. In addition, this approach uses a deep learning framework for continual learning. Continual learning refers to a system's ability to tackle new tasks by utilizing previously acquired knowledge from previous tasks without significantly compromising their prior knowledge. The motivation of the proposed research is to design an efficient framework that helps recognize faces with less facial data and computational resources and ensures that accuracy is maintained.

To recapitulate, the key contributions of the proposed study are the following:

1. The proposed study modified the architecture of the baseline model.

(a) We employed the idea of transfer learning instead of training the CNN model from scratch to obtain the fine-tuned [21] baseline models for the discussed problem.

(b) The architecture of baseline models is modified by concatenating the output feature map of global average pooling (gap) and global max pooling (gmp) [22], FC layer [23], batch normalization (BN) [24], and dropout [25] in the classification layer.

(c) The concept of progressive training is utilized by freezing and unfreezing the model, significantly improving recognition accuracy.

2. The proposed novel hybrid ensemble model: We proposed a novel optimized hybrid ensemble CNN framework (HE-CNN) from the above-discussed fine-tuned baseline models using ensemble learning to improve the recognition rate.
3. Investigated the performance of different face detection algorithms: For face detection, we investigated the performance of two deep learning-based algorithms, single-shot multi-box detector (SSD) [26] and multi-task cascaded convolutional networks (MTCNN), [27] to compare these with traditional algorithms such as Haar feature-based cascade classifier [28] and LBP feature-based cascade classifier [29] using two standard datasets LFW and CPLFW [30], and one self-created criminal dataset.
4. Self-created dataset: Criminal identification is one of the applications of face recognition. Therefore, to demonstrate the real-time application of face recognition, we utilized a small self-created criminal dataset (images collected from the Internet from freely available sources) to recognize criminals. This step involved the collection of images of ten criminals. Mislabeled and vague images from the downloaded images are manually deleted, and 25 images of each class are considered to make a class-balanced dataset. The proposed dataset is available at https://rb.gy/jrjv for research purposes to evaluate the face recognition models.

The research article is classified into five sections. Section 1 discusses a brief overview of the face recognition system and addresses different SOTA. The materials and methods are discussed in Section 2. All the experiments are conducted and analyzed in Section 3. The discussion on conducted experiments is done in Section 4. Finally, we conclude with the research findings and propose the future direction in Section 5.

2 Methods and materials

In this section, we exploited different pre-trained models like ResNet50 [31], VGG16 and VGG19 [32], and DenseNet169 [33] for face recognition tasks and fine-tuned them to acquire the best hybrid model for the addressed task using ensemble transfer learning. The weights of the pre-trained models are procured by the ImageNet challenge dataset [34].

2.1 Datasets used

The authors used two standard datasets, namely LFW and CPLFW, and one small self-created criminal dataset to evaluate SOTA for face detection and recognition. Images of different classes of each dataset are shown in Figure 2.

LFW is a benchmark for face recognition/verification and a publicly available dataset. It was published in 2007 and contained 13,233 images of 5,749 different identities. A total of 1,680 classes having more than one image in the dataset, and 4,096 have only one image in the database. The size of all the images in the dataset is 250×250 with a resolution of 96 DPI (dots per inch), and the image format is JPEG. Most faces are frontal and only consider unconstrained factors such as illumination variation and partial occlusion.

CPLFW is the enhanced version of the LFW standard dataset, considering images with significant pose variations. It was published in 2018 and consisted of 11,652 images of 3,928 individuals containing 2 or 3 images of each class. The accuracy of SOTA for face recognition drops by 15–20% on CPLFW compared to LFW, as it contains images with a considerable variation of unconstrained factors.

The main objective of creating the self-created criminal dataset is the class imbalance in LFW. The largest class contains 500 times more images than those in the lowest class. Due to this drawback, the model could bias toward the class having more images (*i.e.*, the class having more images of the same person could recognize the person accurately, but the class having fewer images of the person could lead to a lower recognition rate). In LFW, unconstrained factors like large pose variation and low-resolution images are not considered. The other reason for preparing the criminal dataset is to consider the low-resolution images, as the images in standard datasets like LFW and CPLFW are captured with high-resolution cameras. There are 10 classes in the proposed dataset labeled with the name of the criminal, and all the classes contain 25 images for training the model to ensure the balance of images in each category. Images of the self-created dataset are taken from the internet, and each image's size is set to 224×224 by taking the average height and width of all images. This dataset is designed to present a real-time face recognition application in video surveillance. The surveillance cameras capture images containing multiple people in a single frame to recognize individuals. Therefore, a set of another 50 images is created for testing the proposed model to recognize many faces at once. These 50 images contain the faces of the 10 criminals and other unknown individuals.

2.2 Proposed modified architecture of baseline models

The early layers of the CNN model extract the features, and the last layers are used for the classification. The architectures of the last layers of the used pre-

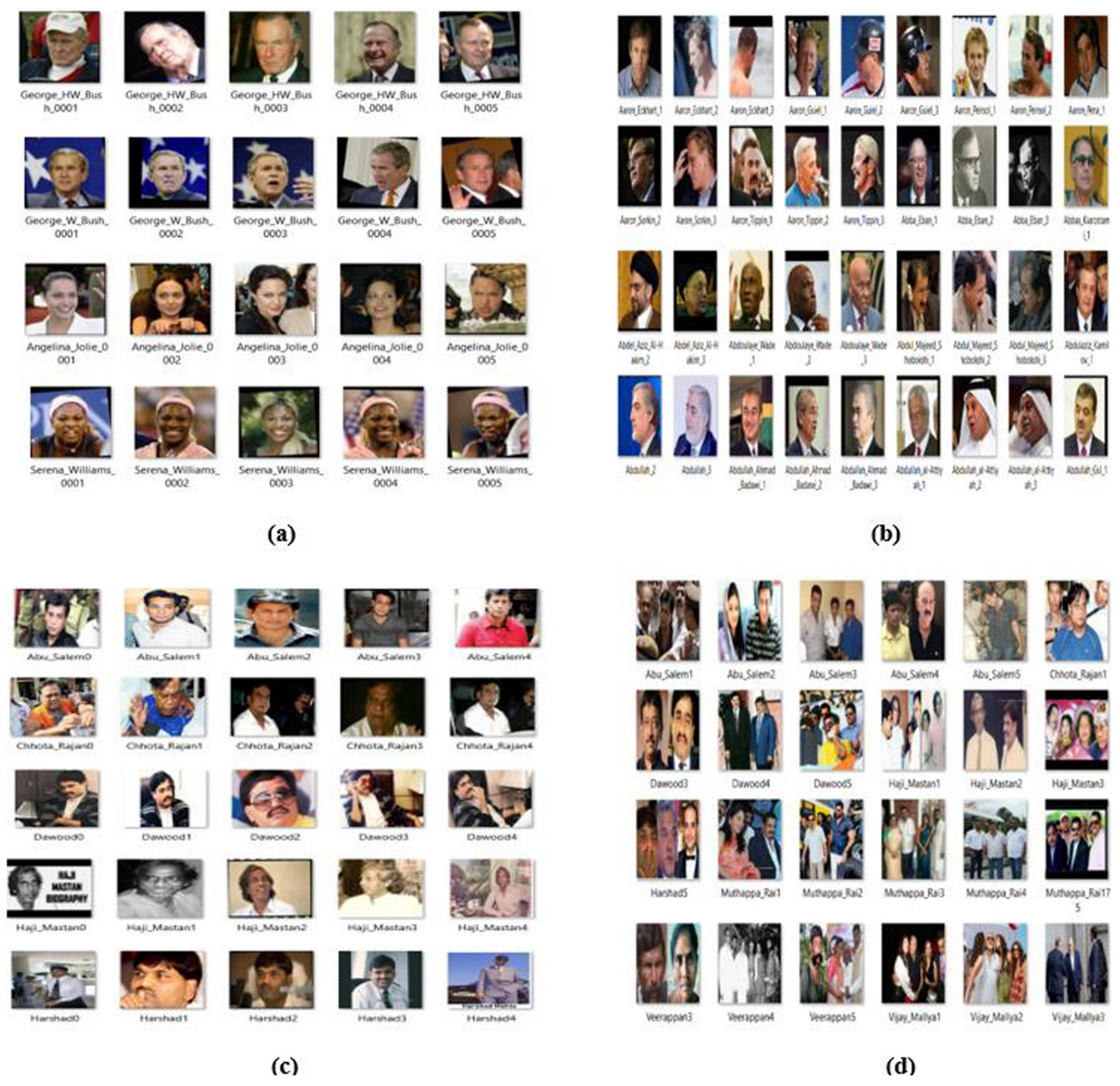

Figure 2: Images of each class of used datasets: (a) LFW, (b) CPLFW, (c) training set of the proposed criminal dataset, and (d) testing set of the proposed criminal dataset.

trained models (VGG, ResNet, DenseNet) are delineated in Figure 3.

In this article, the modified architecture of the base models is proposed by adding global pooling, BN, and dropout in the classification layers of models. The pooling layer helps to abbreviate a large number of trainable parameters from the model. Generally, two types of pooling techniques are used, *i.e.*, average and max pooling, which can be mathematically described using the following equations:

$$P = O_{\max}^{n,n}(F), \tag{1}$$

$$P = O_{\text{avg}}^{n,n}(F), \tag{2}$$

where F is the input feature map received from the previous Conv layer, $O_{\max}^{n,n}(F)$ is the maximum pooling operation on the input feature map of size $n \times n$, $O_{\text{avg}}^{n,n}(F)$ is the average pooling operation, and P is the output of the pooling layer. It is ascertained that sometimes the maximum value of the activation map $n_{\text{H}} \times n_{\text{w}} \times n_{\text{C}}$ (where n_{H} is the height, n_{w} is the width, and n_{C} is the channel count in the feature map) received from the last layers gives better performance than the average value and conversely also true. In order to retain both the maximum and

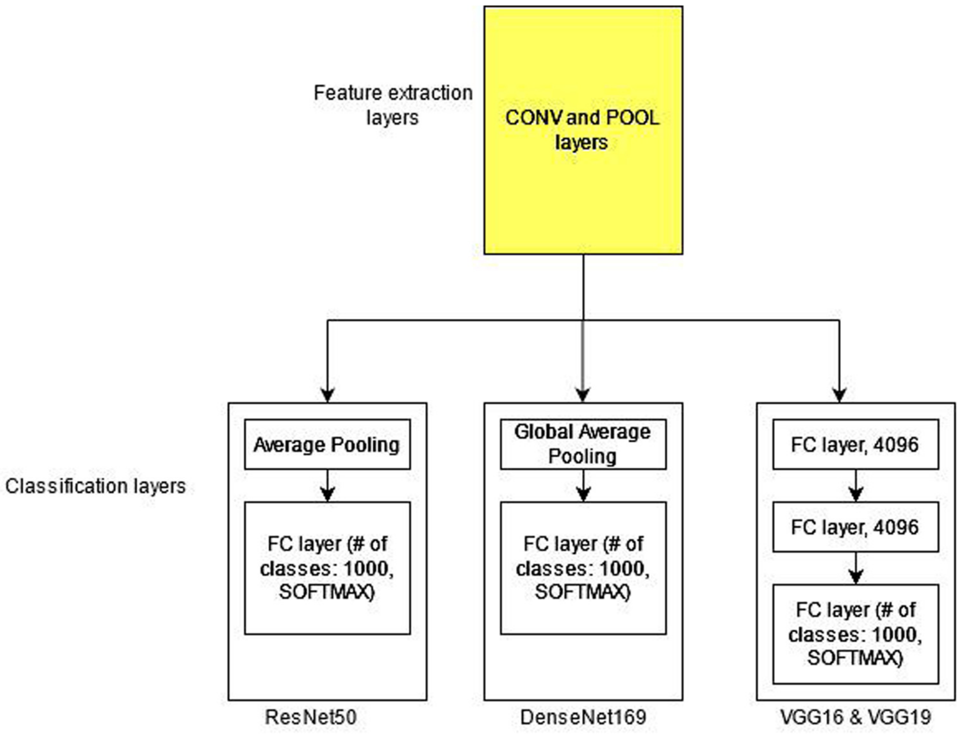
Feature extraction layers
CONV and POOL layers
Classification layers
Average Pooling
FC layer (# of classes: 1000, SOFTMAX)
Global Average Pooling
FC layer (# of classes: 1000, SOFTMAX)
FC layer, 4096
FC layer, 4096
FC layer (# of classes: 1000, SOFTMAX)
ResNet50
DenseNet169
VGG16 & VGG19

Figure 3: The architecture of classification layers of pre-trained models (ResNet50, DenseNet169, VGG16, and VGG19).

average values, we concatenated the max and average values using concatenate function in Keras (https://keras.io). Global pooling helps to reduce each channel in a feature map to a single value and can be used as a substitute for densely connected or FC layers in a classifier. BN effectively normalizes the positive and negative features received from the previous convolutional layer of the model, which helps to reduce the problem of covariate shift [24] and improves accuracy without any side effects [35]. Since we experienced overfitting while training, dropout layers are added for regularization. Dropout is the regularization technique to reduce overfitting. As given in the study of Garbin *et al.* [35], the dropout value can significantly change the model's accuracy. Therefore, different values are considered, and we experimentally acquired the optimal dropout value for the model. The non-linearity functions, such as ReLU [36], PReLU [37], leaky ReLU [38], *etc.*, can be placed before or after the BN layer. In our proposal, the use of leaky ReLU after the BN layer gives better results. Therefore, we used the leaky ReLU activation function because it alleviates the problem of "dying ReLU" [38]. The mathematical expression for calculating the value of leaky ReLU is given in the following equation:

$$f(x) = \max(0.01^{*}x, x). \quad (3)$$

The function produces a value of x when the given input is positive, but if the input is negative, it will output a minimum value of $0.01 \times x$. Therefore, leaky ReLU gives the output for the negative input also. This modification in ReLU leads to a non-zero gradient at the left side of the mathematical graph. In this way, dead neurons will be removed from that region. The modified architecture of the baseline model is shown in Figure 4. The persuasive reasons for the modification in the architecture of baseline models are discussed in Table 1.

2.3 Model training and hyperparameter tuning

In the proposed approach, model training is done in the following two steps.

Step 1: First, freeze the early layers in the network and train only classification layers. However, the initial layers (*i.e.*, the feature extraction layers) are not trained during the first step of training the network.

Step 2: Then, a fine-tuned model is loaded from step 1, and all the layers are unfreezed to train the complete model. Figure 5 provides a visual representation of the entire procedure.

The model's training process involves implementing a one-cycle policy [39], which replaces the fixed learning rate with cyclical learning rates. Hyperparameter tuning has proven to be an effective solution to improve machine learning model accuracy. In the conferred approach,

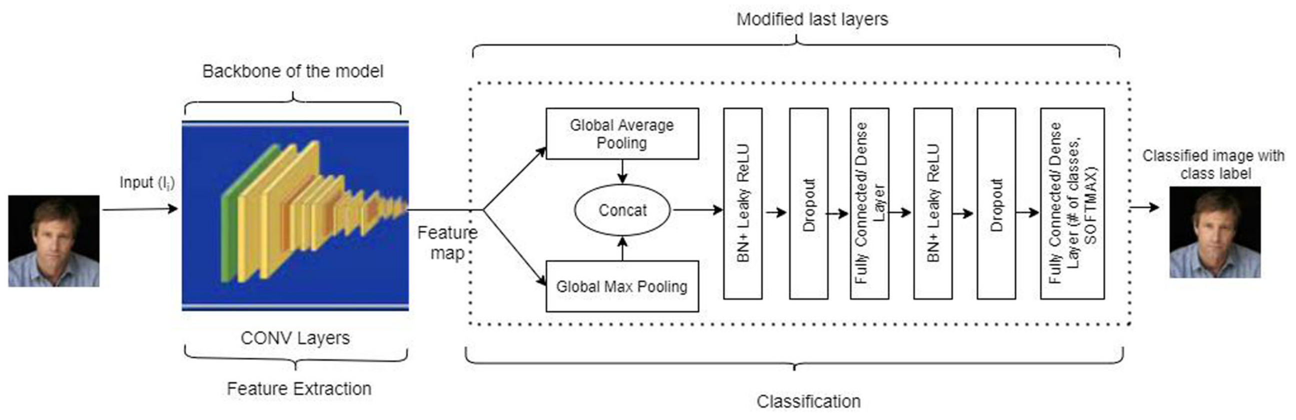

Figure 4: The modified architecture of the baseline model consisting of gmp, gap, BN, dropout, and FC layers (the dotted line shows the modified part of the model).

tweaking of the learning rate, batch size, image size, epoch, and drop-out is done experimentally in Section 3.2 to tune the pre-trained models for the addressed task. The selection of learning rate should be chosen wisely; if it is too large, the optimal value may be an overshoot, and if it is too small, it will require too many iterations to converge to the best value. Therefore, the learning rate finder (LRF) curve [39] is used to locate the optimal learning rate for the model. The LRF is a valuable tool for automatically determining a reasonable learning rate for any model. For example, the red dot in Figure 6 illustrates the optimal learning rate for the deep learning model. The learning rate is gradually raised from an exponentially low value (*e.g.*, 10^{-6}) to a high value (*e.g.*, 1) while training the data in small batches. During the cool-down phase, the training rate oscillates between a lower and higher learning rate boundary before returning to its initial low boundary. A one-hot vector is created through conversion to predict the class of data while employing categorical cross-entropy as the loss function in Eq. (4) within the softmax layer:

$$L(\Theta) = -\frac{1}{n}\sum_{i=1}^{n}\sum_{j=1}^{C}[y_{ij}\log(p_{ij})], \tag{4}$$

where n is the count of images in training data, i is the index of the input image (*i.e.*, ith image), j is the class's index, y_{ij} is the one-hot encoded label, and p_{ij} is the probability distribution over C classes. Adam [40] optimizer is used for the optimization of the model.

2.4 Proposed HE-CNN framework

Algorithm 1 acquires the optimized baseline models and utilizes the ensemble learning approach to get an efficacious hybrid model. Ensemble learning combines the predictions of more than one model to produce the optimal predictive model for the addressed task. The stacking approach of ensemble learning is used to design a hybrid model for the face recognition problem. The final prediction of the hybrid model is made by aggregating the results obtained from the fine-tuned baseline models by conducting a weighted sum operation. The weighted sum or weighted average [41] operation is often applied to ensemble models to give more importance to the predictions of the better-performing models. The idea behind the weighted sum operation is to assign different weights to the predictions of each model in the ensemble based on their relative performance on a validation set. The better-performing models are given higher weights, while the poorer-performing models are assigned lower weights. This means that the final prediction of the ensemble will be more influenced by the predictions of the better models and less influenced by the predictions of the poorer models. Using a weighted sum operation on ensemble models, we can leverage the strengths of multiple models and minimize their weaknesses. This can lead to better overall performance and more robust predictions [42]. The predicted face using the hybrid ensemble model ($P_{\text{HE-CNN}}$) is defined in Eq. (5). VGG19 shows better accuracy in Tables 3 and 5. As a result, the VGG19 version is chosen above the VGG16 variant. However, we considered VGG19, DenseNet169, and ResNet50 in the hybrid model. The complete procedure is shown in Figure 7:

$$P_{\text{HE-CNN}} = \sum_{i=1}^{\S} W_i \sum_{j=1}^{n} \frac{1}{\sum_{k=1}^{C} e^{\theta_k^T f^{(j)}}} \begin{pmatrix} e^{\theta_1^T f^{(j)}} \\ \cdots \\ e^{\theta_C^T f^{(j)}} \end{pmatrix}, \tag{5}$$

where W_i denotes the weight of rectified baseline models, § = 3 because we considered three models for the ensemble framework, n is the count of image samples in training data, C is the number of classes in a dataset, $f^{(j)}$ is the feature of the jth sample, θ is the parameter matrix of the

Table 1: Persuasive reasons for the rectification of the classification layers of baseline models

Characteristics	Standard ResNet50	Standard VGG19	Standard DenseNet169	Rectified architecture	Persuasive reasons for the rectification
Pooling layer	Average pooling	No pooling layer	Global average pooling	Concatenation of gap and gmp	The activation map derived from the preceding layer may exhibit superior performance to its mean value, and the converse is also true
No. of fully/densely connected (FC) layer	1	3	1	2	A stronger network that facilitates improved representation and learning of the intermediary characteristics is generated by using an additional layer in ResNet and DenseNet and removing an extra layer from VGG
Linear activation	ReLU	ReLU	ReLU	Leaky ReLU	To address the issue of dying ReLU
Regularization	No dropout	No dropout	No dropout	The dropout layer is used	To minimize the overfitting issue

softmax loss function $L(\theta)$, and $\theta_k^T f^{(j)}$ is the inner product of θ_k and $f^{(j)}$. The optimal values of W_1, W_2, and W_3 are selected using VotingClassifier available in the scikit-learn library of Python (https://rb.gy/p0ig).

Algorithm 1: Algorithm of the proposed approach for training to obtain fine-tuned models

```
Input: Training Dataset $D = \{x_i, y_i\}_{i=1}^{n}$, where $n$ is the count of input images in the dataset
    Pre-trained CNN model (here, VGG16, VGG19, ResNet50 and DenseNet169 are taken)
    No. of epochs ($e$)
    Batch size ($\alpha$)
    Image size ($m$)
    Calculated optimal learning rate using LRF curve ($\eta$)
Output: Fine-tuned best CNN model for the addressed task (output_tuned_model).
  function TL_step 1 (D, CNN, n, $\alpha$, m, $\eta$)
    first train head and freeze the remaining layers
    parameters ← load_model(CNN, train_head=True)
      repeat
        for all ($x_i$, $y_i$) ϵ D do
        activation ← forward_propagation ($x_i$, parameters)
        cost ← Loss_function(activation, $y_i$)
        gradient ← back_propagation(activation, cost)
        parameters ← weight_update(parameters, gradient, $\eta$)
            end for
        until e times
    return tuned_model
    function TL_step2(D, tuned_model, n, $\alpha$, m, $\eta$)
        Unfreeze all the remaining layers and train the entire model
        Load model received from function TL_step1 (i.e., tuned_model)
        parameters ← load_model(tuned_model, train_head=False)
      repeat
        for all ($x_i$, $y_i$) ϵ D do
        activation ← forward_propagation ($x_i$, parameters)
      cost ← Loss_function(activation, $y_i$)
      gradient ← back_propagation(activation, cost)
      parameters ← weight_update(parameters, gradient, $\eta$)
        end for
        until e times
    return output_tuned_model
```

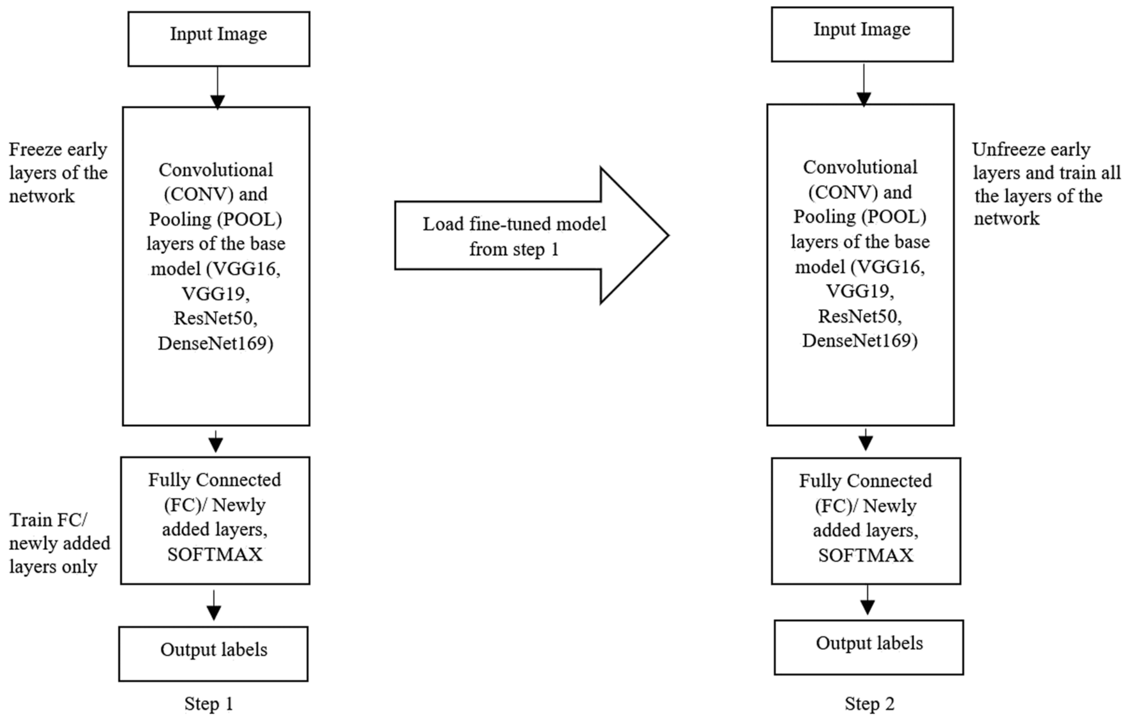
Input Image
Freeze early layers of the network
Convolutional (CONV) and Pooling (POOL) layers of the base model (VGG16, VGG19, ResNet50, DenseNet169)
Train FC/ newly added layers only
Fully Connected (FC)/ Newly added layers, SOFTMAX
Output labels
Step 1
Load fine-tuned model from step 1
Input Image
Unfreeze early layers and train all the layers of the network
Convolutional (CONV) and Pooling (POOL) layers of the base model (VGG16, VGG19, ResNet50, DenseNet169)
Fully Connected (FC)/ Newly added layers, SOFTMAX
Output labels
Step 2

Figure 5: Steps for training the models.

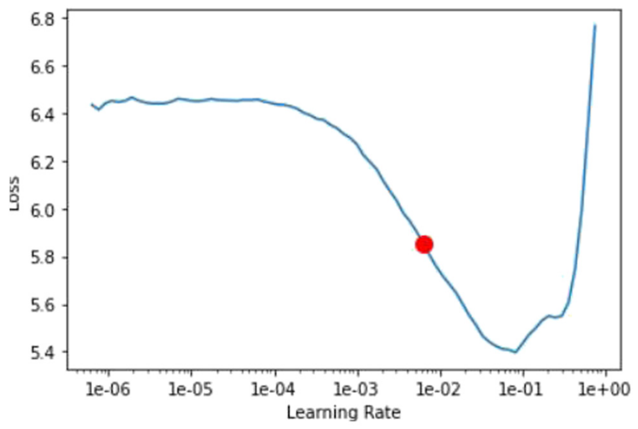

Figure 6: The LRF curve.

3 Results

To assess the effectiveness of face detection and recognition models, experiments were conducted independently. After thorough evaluation and comparison with other approaches in Section 3.2, SSD was selected to detect and align faces for the recognition phase, despite extensive research on face detection. Our system is configured with Windows 10, one Nvidia Tesla with K40, and 16 GB memory. The TensorFlow (https://www.tensorflow.org/) version is 2.4.0, while Keras and OpenCV [43] are 2.4.3 and 4.5.1, respectively.

3.1 Evaluation parameters to assess face detection and recognition algorithms

We considered three evaluation parameters for the assessment of face detection algorithms: true positive rate (TPR), false positive rate (FPR), and false negative rate (FNR) [44]. TPR can also be called recall or sensitivity. It determines all the significant instances of the classification model. The model with no false-negative contains the recall value as 1. FPR is the total count of false-negative assessments divided by the number of all negative evaluations. Another term for FNR is the miss rate. It gives the proportion of correct results, which were misclassified as incorrect. The estimation of the values of TPR, FPR, and FNR is done using Eqs. (6)–(8), where TP relates as having both the actual and predicted label the same. For example, an image contains a face, and the algorithm detects it as a face. FP is defined as the true label is not a face, but the predicted label is a face. FN has the true label of a face, but the predicted label does not have a face.

$$\text{Recall or TPR} = \frac{\text{TP}}{\text{TP} + \text{FN}}, \tag{6}$$

$$\text{FPR} = \frac{\text{FP}}{\text{FP} + \text{TN}}, \tag{7}$$

$$\text{FNR} = \frac{\text{FN}}{\text{FN} + \text{TP}}. \tag{8}$$

Table 2: Scores of various face detection models

Face detection models, proposed year	CPLFW			LFW			Criminal dataset		
	TPR (%)	FPR (%)	FNR (%)	TPR (%)	FPR (%)	FNR (%)	TPR (%)	FPR (%)	FNR (%)
SSD, 2016	**96.9**	1.4	**1.7**	**99.8**	0.2	**0**	**97.9**	0.7	**1.4**
MTCNN, 2016	96.3	1.2	2.5	99.3	0.6	0.1	96.2	1	2.8
Haar cascade (Viola Jones), 2004	53.9	0.5	45.6	98.4	0.6	1	60	2	38
LBP cascade, 2006	44.2	0.7	55.1	94.3	0.8	4.9	47	1	52

The bold value means the best value in comparison to other methods.

Two benchmark datasets and one self-created dataset are exerted to assess the efficacy of the discussed architecture in this study. The description of the discussed datasets is given in Section 2.1. The performance of the discussed technique and other SOTA for all datasets mentioned is measured by the classification accuracy evaluation parameter, which is determined using the following equation:

$$\text{Accuracy} = \frac{\text{Number of correctly recognized images}}{\text{Total number of images}}. \quad (9)$$

To evaluate the classification model [44], other measures such as precision, recall, and error rate are employed. This is because relying solely on accuracy to determine the best classifier can be insufficient due to what is known as the accuracy paradox [45]. Precision refers to the proportion of true positives concerning predicted positives. Eqs. (10) and (6) provide the formulae for deriving precision and recall. In addition, the total number of inaccurate predictions on the test set divided by all of the test set predictions can be used to compute the error rate given in Eq. (11). We can always determine the accuracy from the error rate since they are complementary quantities:

$$\text{Precision} = \frac{\text{Truly positives}}{\text{Predicted positives}}, \quad (10)$$

$$\text{Error rate} = \frac{\text{Number of incorrect predictions}}{\text{Total number of images}}. \quad (11)$$

Table 3: Training and validation loss of pre-trained models (VGG16, VGG19, ResNet50, and DenseNet169) and modified pre-trained models with PC in LFW

Model	TH = T/F	E	LR	TL	VL	ER	TA	VA	*P*	*R*
Pre-trained models										
VGG16	—	30	1×10^{-2}	0.3234	0.6900	0.2014	0.9254	0.7985	0.8260	0.7962
VGG19	—	30	1×10^{-2}	0.3699	0.9814	0.2716	0.9173	0.7283	0.8281	0.7257
ResNet50	—	30	1×10^{-2}	0.2501	0.6230	0.1692	0.9221	0.8307	0.8602	0.8327
DenseNet169	—	30	1×10^{-2}	0.2107	0.7527	0.1886	0.9234	0.8113	0.8626	0.8125
Modified pre-trained models with PC										
Modified VGG16	T	15	1×10^{-2}	0.1932	0.1739	0.0512	0.9345	0.9487	0.9490	0.95011
	F	30	1×10^{-6}, 8×10^{-5}	**0.0642**	**0.0783**	**0.0228**	**0.9812**	**0.9771**	**0.9771**	**0.9779**
Modified VGG19	T	15	1×10^{-2}	0.2115	0.2047	0.0644	0.9335	0.9355	0.9357	0.9350
	F	30	1.1×10^{-5}, 1×10^{-4}	**0.0140**	**0.0438**	**0.0135**	**0.9914**	**0.9864**	**0.9864**	**0.9866**
Modified ResNet50	T	15	2.09×10^{-3}	0.2099	0.2416	0.0750	0.9315	0.9249	0.9247	0.9263
	F	30	1.91×10^{-6}, 8×10^{-5}	**0.0311**	**0.0783**	**0.0238**	**0.9901**	**0.9761**	**0.9763**	**0.9768**
Modified DenseNet169	T	15	1×10^{-2}	0.0288	0.0560	0.0150	0.9964	0.9849	0.9845	0.9849
	F	30	1.32×10^{-6}, 1×10^{-5}	**0.0182**	**0.0453**	**0.0115**	**0.9987**	**0.9884**	**0.9882**	**0.9883**

PC, proposed classifier; TH, Train_head; E, epoch; LR, learning rate; TL, training loss; VL, validation loss; ER, error rate; TA, training accuracy; VA, validation accuracy; P, precision; R, recall.
The bold values mean the best values in comparison to other comparing methods.

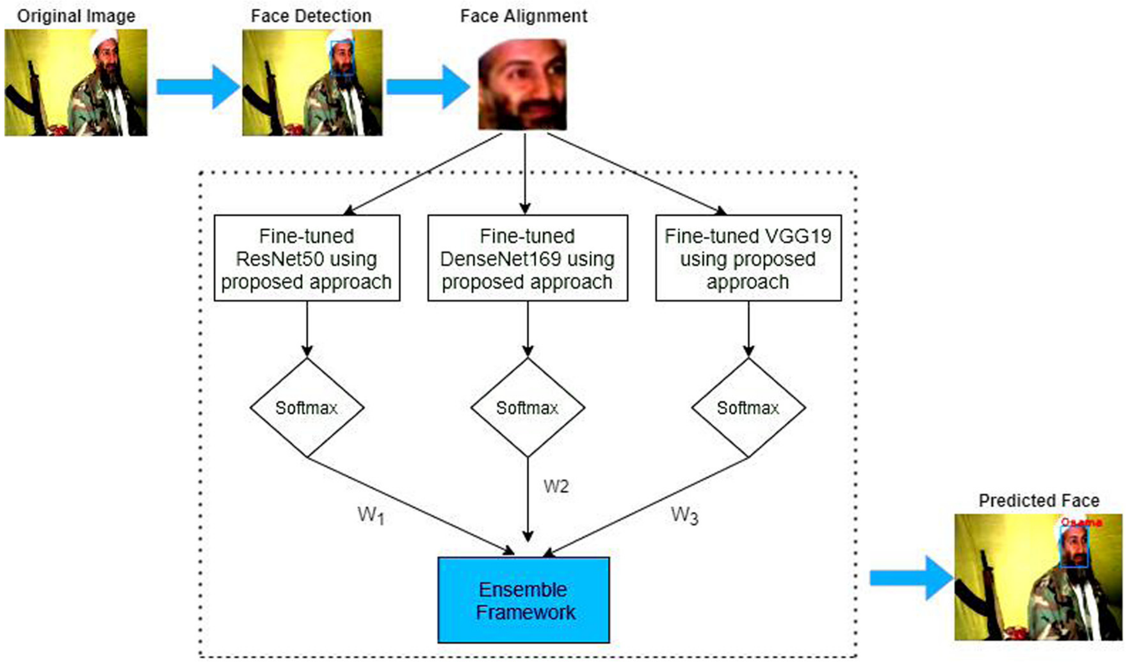
Original Image
Face Detection
Face Alignment
Fine-tuned ResNet50 using proposed approach
Fine-tuned DenseNet169 using proposed approach
Fine-tuned VGG19 using proposed approach
Softmax
Softmax
Softmax
W1
W2
W3
Ensemble Framework
Predicted Face
Osama

Figure 7: The proposed HE-CNN framework.

3.2 Face detection and recognition results

The implementation of the Haar feature and LBP feature-based face detectors rely on OpenCV, while MTCNN and SSD are available as a package in Python (https://pypi.org/project/mtcnn/, https://pypi.org/project/ssd/). Table 2 delineates the collation between the accuracy of the employed face detection models. We used the same datasets for both addressed tasks, such as detection and recognition of the face, but the ground truth bounding box annotation is not available in the dataset for evaluating face detection algorithms. Therefore, we experimentally filtered the images in which the algorithm detected no face and more than one face and manually found false positives and negatives.

The tweaking of hyperparameter values used in the proposed methodology is done after rigorous experiments. The value of the learning rate is set to its optimal value with the help of the LRF curve that varies with the model and dataset. The batch size and image size for all the experiments are taken as 128 and 120 × 120, respectively, for a fair comparison. Keras does not support the loss graph over batches, so we implemented a customized callback (https://rb.gy/au69) to get the graph of loss *vs* batches to visualize the variation of training and validation loss concerning batches. In Tables 3 and 5, Train_head = T (True) means training of head only and the remaining layers are freezed, while Train_head = F (False) means that all the layers are unfreezed, and training is done for the complete model. When training the head while the remaining layers are freezed, the total number of epochs considered for training is 15. Otherwise, 30 epochs are taken when there is a training of the complete model (*i.e.*, the second step of training) in LFW, while 7 and 15 epochs are taken for CPLFW

Table 4: Comparison of the proposed work with other SOTA in the LFW dataset

Author, year of publication	Techniques used	Accuracy (%)	Error rate (%)
Sun *et al.*, 2014 [11]	DeepID	97.45	2.55
Parkhi *et al.*, 2015 [12]	Deep CNN	98.95	1.05
Wen *et al.*, 2016 [15]	Combination of softmax loss and center loss with CNN	99.28	0.72
Kang, 2019 [47]	Self-learning CNN	94.9	5.1
Ben Fredj *et al.*, 2020 [48]	GoogleNet + Data augmentation	99.2	0.8
Mishra and Singh, 2022 [49]	Deep learning architectures + Hardmining loss	95.55	4.45
Proposed approach	The hybrid model of the fine-tuned pre-trained models using ensemble learning (HE-CNN)	**99.35**	**0.65**

Table 5: Training and validation loss of pre-trained models (VGG16, VGG19, ResNet50, and DenseNet169) and modified pre-trained models with PC in CPLFW

Model	TH = T/F	E	LR	TL	VL	ER	TA	VA	*P*	*R*
Pre-trained models										
VGG16	—	15	1×10^{-3}	**0.1580**	**0.6419**	**0.1215**	**0.9634**	**0.8784**	**0.8711**	**0.8734**
VGG19	—	15	1×10^{-3}	0.1623	0.6357	0.1280	0.9563	0.8719	0.8654	0.8724
ResNet50	—	15	1×10^{-3}	0.0678	0.4507	0.0905	0.9856	0.9094	0.9001	0.9054
DenseNet169	—	15	1×10^{-3}	0.0501	0.4378	0.0887	0.9898	0.9112	0.9200	0.9198
Modified pre-trained models with PC										
Modified VGG16	T	7	2.75×10^{-2}	1.1628	0.9759	0.2077	0.7734	0.7922	0.7792	0.7986
	F	15	6.31×10^{-7}, 1×10^{-5}	0.8944	0.8895	0.1896	0.8112	0.8103	0.8264	0.8164
Modified VGG19	T	7	1.1×10^{-2}	1.4396	1.2920	0.2603	0.7243	0.7396	0.7256	0.7345
	F	15	1×10^{-5}, 5×10^{-4}	**0.2921**	**0.4468**	**0.0844**	**0.9323**	**0.9155**	**0.9166**	**0.9132**
Modified ResNet50	T	7	1.32×10^{-2}	0.5944	0.6587	0.1314	0.8867	0.8685	0.8764	0.8678
	F	15	2.2×10^{-6}, 1×10^{-4}	**0.2334**	**0.4462**	**0.0849**	**0.9458**	**0.9150**	**0.9245**	**0.9152**
Modified DenseNet169	T	7	1.32×10^{-2}	0.4330	0.4568	0.0879	0.9198	0.9120	0.9132	0.9134
	F	15	5×10^{-6}, 5×10^{-5}	**0.2227**	**0.3583**	**0.0842**	**0.9289**	**0.9157**	**0.9234**	**0.9219**

PC, proposed classifier; TH, Train_head; E, epoch; LR, learning rate; TL, training loss; VL, validation loss; ER, error rate; TA, training accuracy; VA, validation accuracy; P, precision; R, recall.
The bold values mean the best values in comparison to other comparing methods.

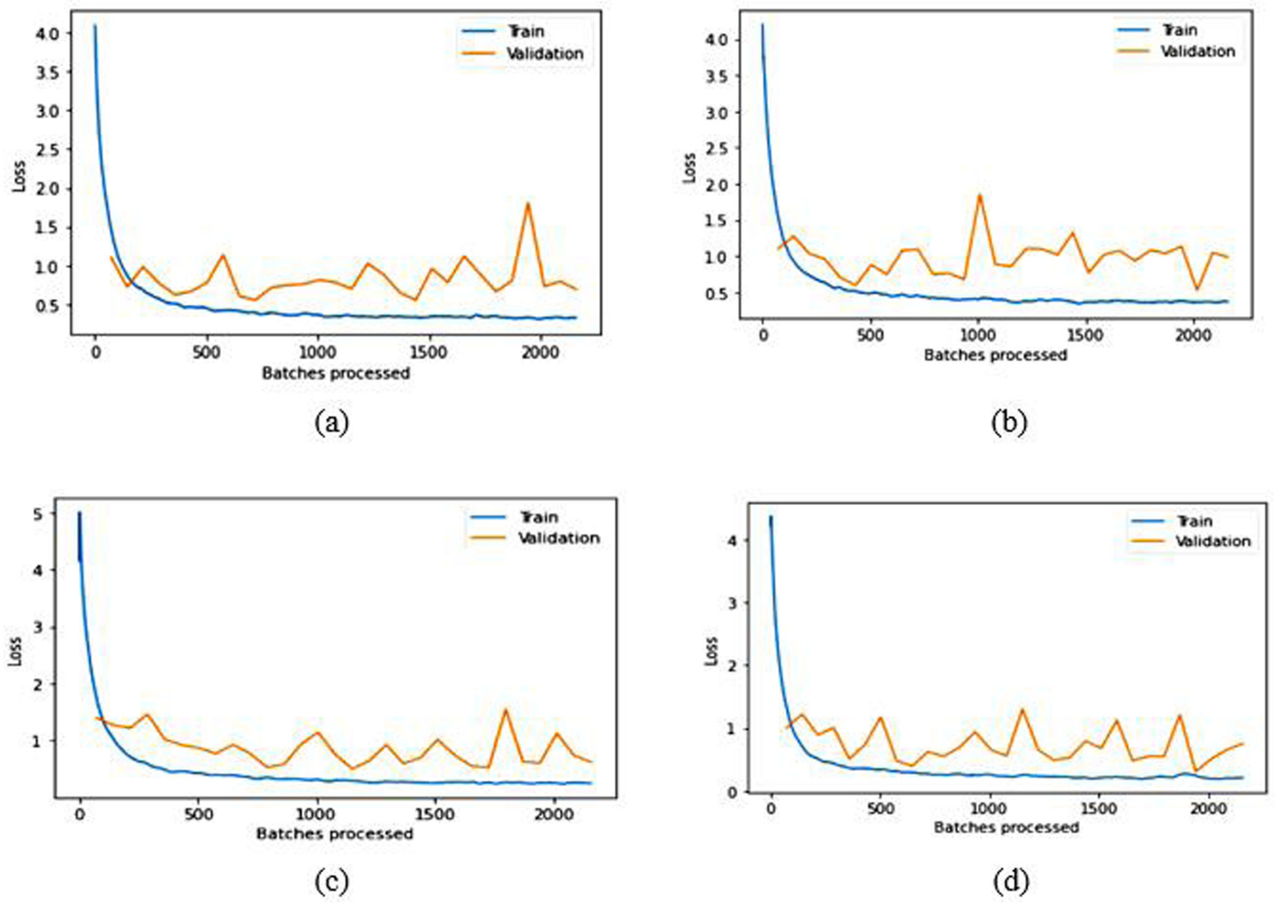

Figure 8: Training and validation loss over batches processed graphs for pre-trained (a) VGG16, (b) VGG19, (c) ResNet50, and (d) DenseNet169 in the LFW dataset.

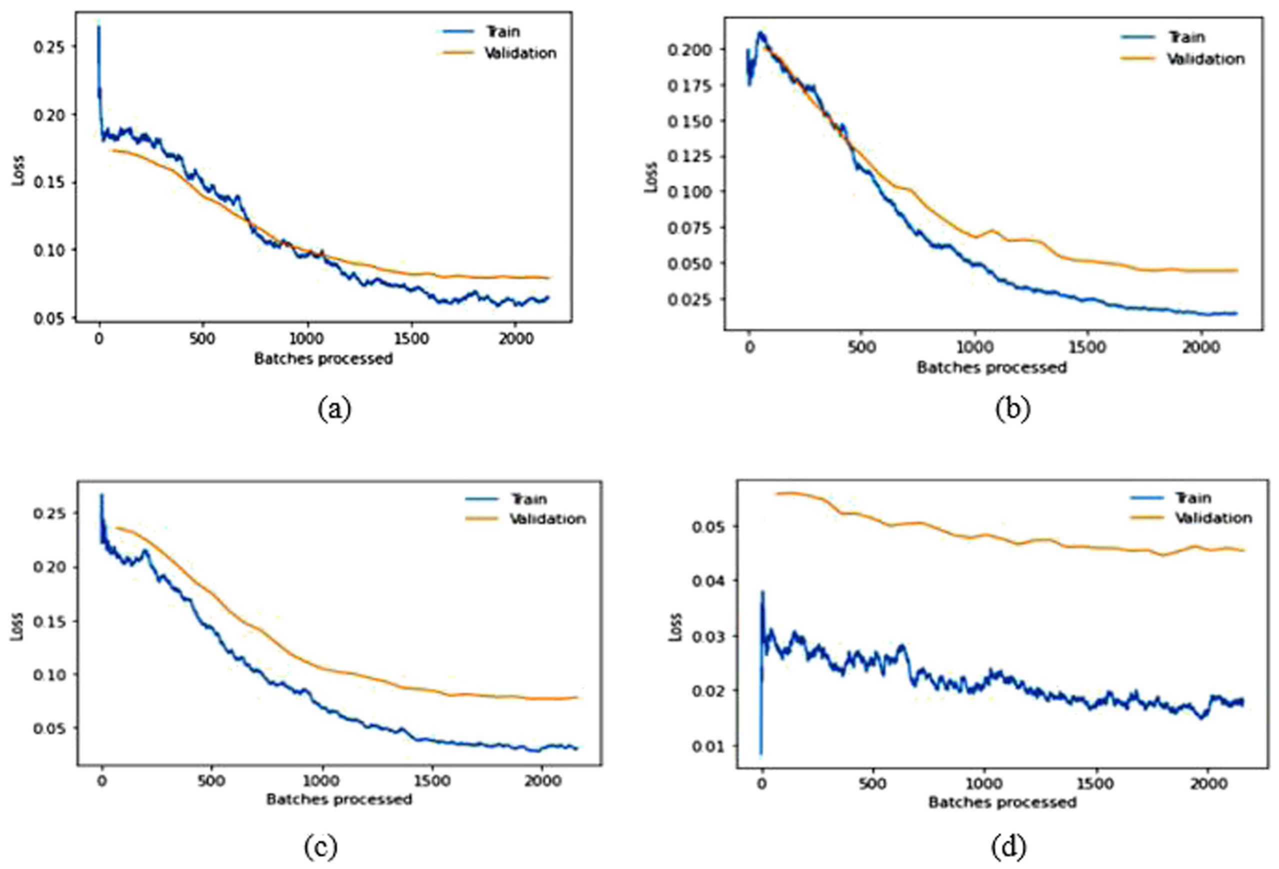

Figure 9: Training and validation loss over batches processed graphs for modified (a) VGG16, (b) VGG19, (c) ResNet50, and (d) DenseNet169 in the LFW dataset.

during training. After obtaining the fine-tuned models, ensemble learning is utilized to design the hybrid model (HE-CNN) to achieve better accuracy.

3.2.1 Experimental results on the LFW dataset

The split ratio of the dataset used in the experiment is 7:3, *i.e.*, 70% of the samples in the dataset are used for training and 30% are used for validation. Section 2.1 provides an in-depth overview of the dataset. The classes containing more than one sample are considered for experimental evaluation (*i.e.*, 1,680 classes are considered). Data augmentation [46], known as oversampling, is utilized through a series of standard transformations such as vertical flip, horizontal flip, rotation, zooming, warping, scaling, and lighting to ensure balance in the considered classes. The total number of considered images for experimental evaluation is 13,440 after data augmentation (*i.e.*, 9,408 are used for training and 4,032 are used for validation). Dropout values are set to 0.1 and 0.2 for the layers used in the modified architecture. Training and

Table 6: Comparison of the proposed work with other SOTA in the CPLFW dataset

Author, year of publication	Techniques used	Accuracy (%)	Error rate (%)
Liu *et al.*, 2017 [50]	SphereFace	81.4	18.6
Cao *et al.*, 2018 [51]	VGGFace2	84	16
Liu *et al.*, 2021 [52]	Lightweight CNN	89.52	10.48
Proposed approach	Hybrid model of the fine-tuned pre-trained models using ensemble learning	**91.58**	**8.42**

The bold value means the best value in comparison to other methods.

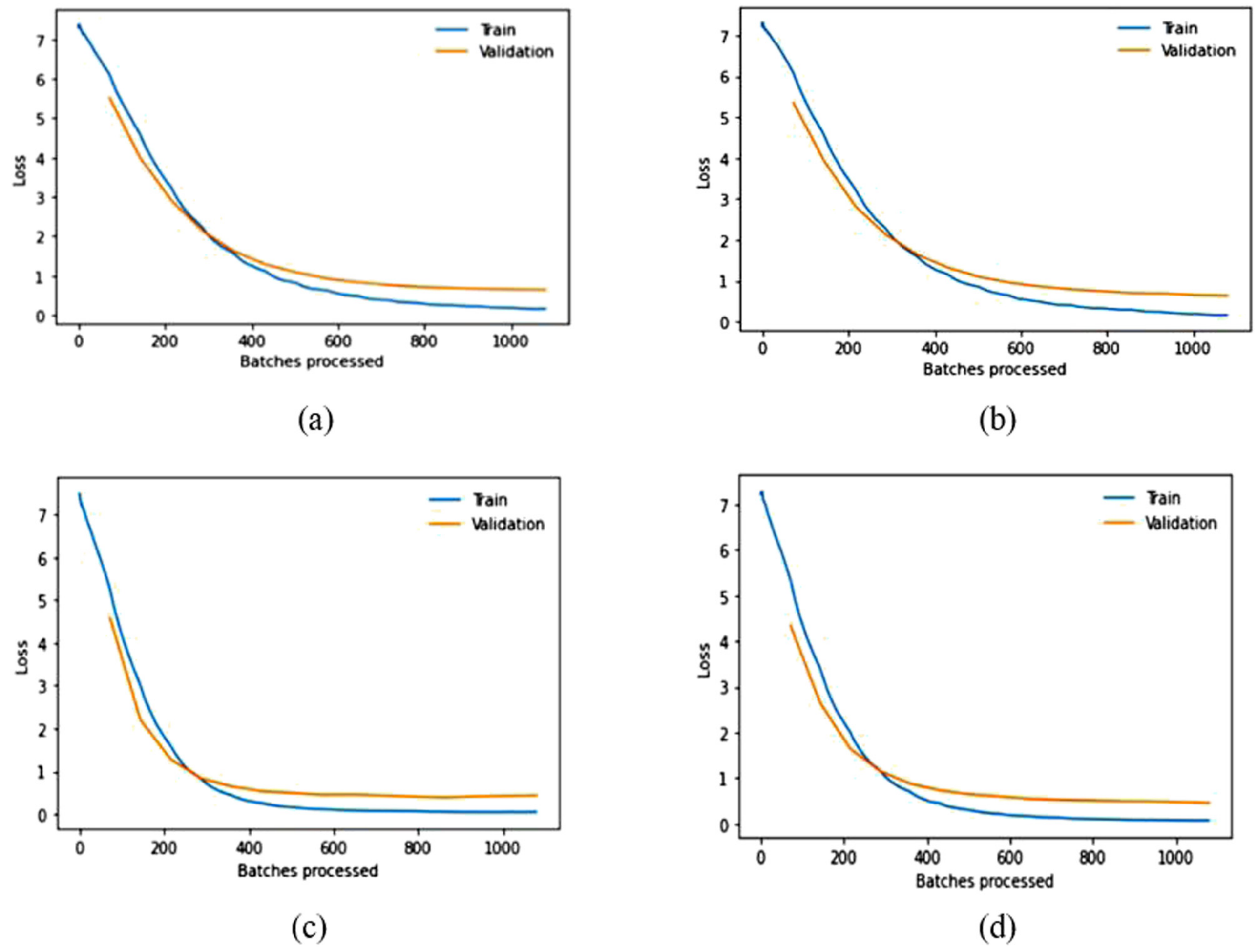

Figure 10: Training and validation loss over batches processed graphs for pre-trained (a) VGG16, (b) VGG19, (c) ResNet50, and (d) DenseNet169 in the CPLFW dataset.

validation losses for different models are illustrated in Tables 3 and 4; they list the comparison of the intended approach with other existing techniques. The learning rate is chosen randomly for pre-trained models, while modified pre-trained models utilize the learning rate identified through the LRF curve. Figures 8 and 9 illustrate the training and validation loss over batches processed of pre-trained and modified pre-trained models, respectively.

3.2.2 Experimental results on the CPLFW dataset

In this experimental evaluation, random splitting of the CPLFW dataset is done with a splitting ratio of 8:2 (*i.e.*, 80% of images [9,322] are used for training and 20% [2,330] are used for validating the model). The dropout values are set to 0.25 and 0.5. Training and validation losses for different models are shown in Table 5. The comparison of the proposed approach with other existing techniques is listed in Table 6. Finally, the training and validation loss over batches processed graphs for the pre-trained and fine-tuned baseline models are delineated in Figures 10 and 11.

3.2.3 Experimental results on the self-created criminal dataset

A small criminal dataset is created containing 25 images of each class of criminals, namely Haji Mastan, Vijay Mallya, Dawood, Harshad, Osama, Veerappan, Chhota Rajan, Muthappa Rai, Abu Salem, and Vikas Dubey, by downloading these images from the internet to demonstrate the real-time application of face recognition. Mislabeled and vague images from the downloaded images are manually deleted and 25 images of each class are considered to make a class-balanced dataset. Data augmentation, known as the oversampling technique, is utilized to expand the count of samples in each class. In order to maintain the balance of the class, images in individual classes are

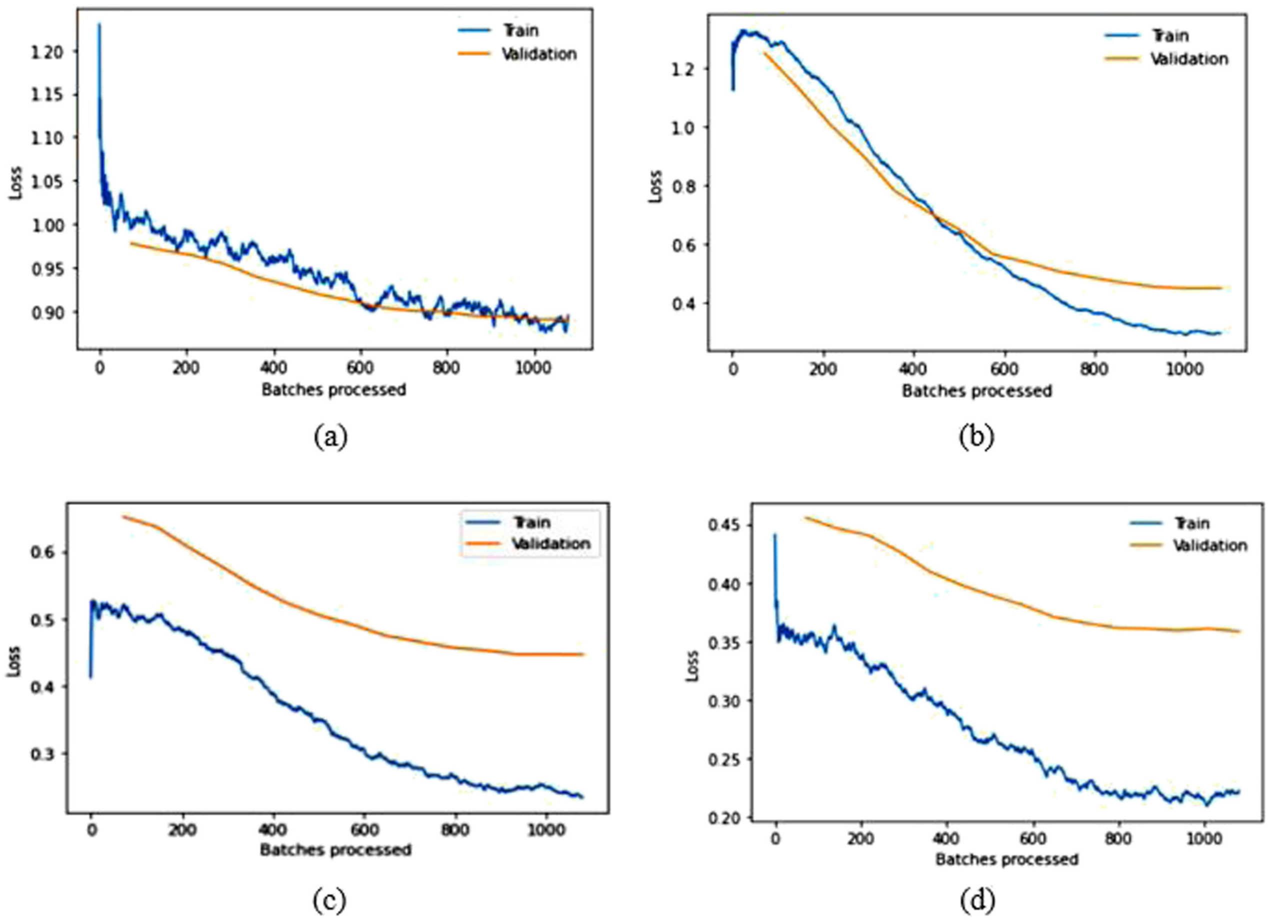

Figure 11: Training and validation loss over batches processed graphs for modified (a) VGG16, (b) VGG19, (c) ResNet50, and (d) DenseNet169 in the CPLFW dataset.

augmented to generate 50 samples using a set of transformations, such as vertical flip, horizontal flip, mirroring, warping, scaling, rotation, zooming, and lighting. The dataset is divided into two sets consisting of 80 and 20% samples (*i.e.*, 400 samples of the dataset are considered for training and 100 samples are taken for testing). Testing on a self-created dataset is done in two ways. First, the testing is done using 100 random samples from 500 images. The accuracy of the proposed hybrid model on a self-created dataset is 95%, while the precision score, recall score, and error rate are 0.954167, 0.952393, and 5%, respectively. The confusion matrix to analyze the correct results present in the diagonal of the matrix is delineated in Figure 12.

Second, another testing dataset contains 50 images with more than one face to demonstrate the real-time surveillance results. The set of 50 images is distinct from the collection of 500 images but consists of the faces of the same 10 criminals and other unknown individuals. As the testing images contain more than one face, the recognition rate of the proposed technique in the criminal dataset is calculated by manually analyzing each image, as shown in Figure 13, achieving 87% recognition accuracy.

4 Discussion

The results in Table 2 demonstrate that SSD outperforms other face detection algorithms in terms of TPR while exhibiting a lower FNR on the datasets discussed earlier. SSD has an advantage in terms of efficiency and can detect even significantly blur faces, which is the main challenging factor in video surveillance. Therefore, we used the SSD in the detection step of face recognition. Based on the experimental findings regarding facial recognition algorithms, relying solely on pre-trained models is inadequate for achieving optimal accuracy.

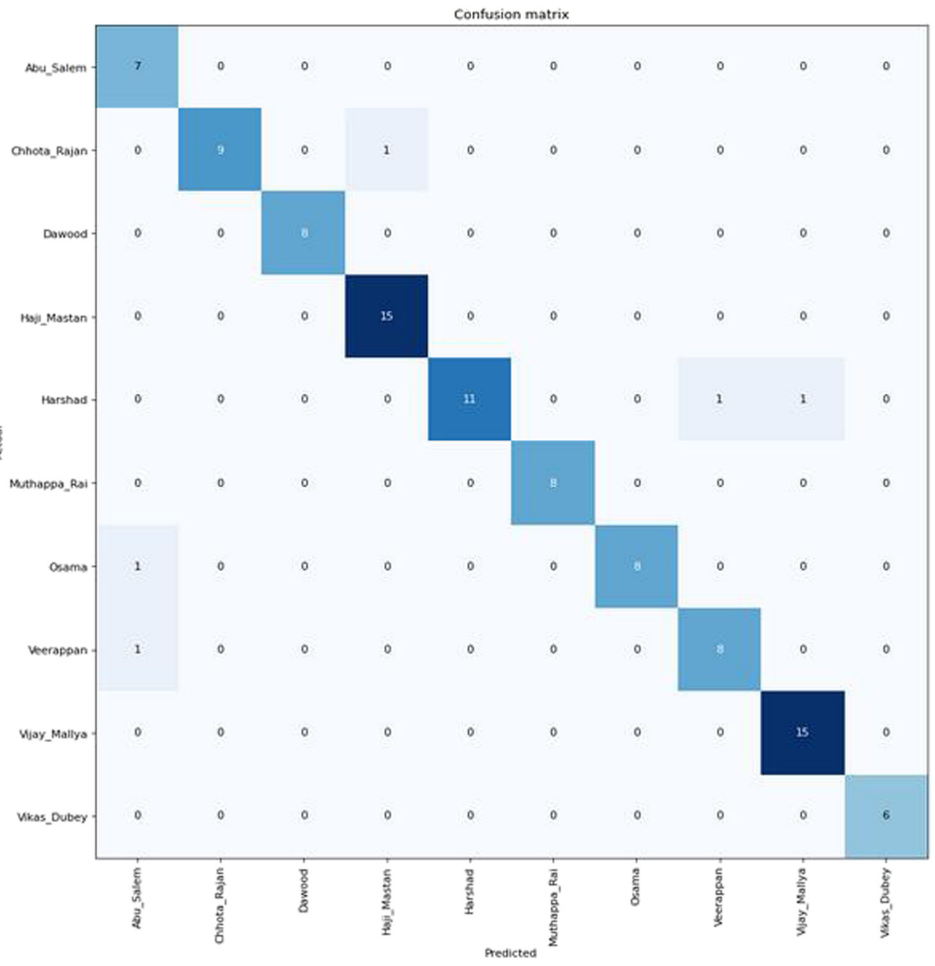

Actual \ Predicted	Abu_Salem	Chhota_Rajan	Dawood	Haji_Mastan	Harshad	Muthappa_Rai	Osama	Veerappan	Vijay_Mallya	Vikas_Dubey
Abu_Salem	7	0	0	0	0	0	0	0	0	0
Chhota_Rajan	0	9	0	1	0	0	0	0	0	0
Dawood	0	0	8	0	0	0	0	0	0	0
Haji_Mastan	0	0	0	15	0	0	0	0	0	0
Harshad	0	0	0	0	11	0	0	1	1	0
Muthappa_Rai	0	0	0	0	0	8	0	0	0	0
Osama	1	0	0	0	0	0	8	0	0	0
Veerappan	1	0	0	0	0	0	0	8	0	0
Vijay_Mallya	0	0	0	0	0	0	0	0	15	0
Vikas_Dubey	0	0	0	0	0	0	0	0	0	6

Figure 12: Confusion matrix for the testing of 100 images.

Some modifications need to be implemented to improve the recognition accuracy of the models. After obtaining fine-tuned-modified baseline models, ensemble learning can be utilized to get SOTA competent recognition rate in LFW and CPLFW, as illustrated in Tables 4 and 6. The original pre-trained models are trained on ImageNet, comprising 1,000 classes. However, the number of classes mentioned in the last FC layer of the pre-trained models is insignificant in our experiments. Therefore, the approach in this article modified only the last FC layer to mention the count of classes of the used datasets for the experimental evaluation given in Tables 3 and 5. The above results and graphs show that the pre-trained models, without any modification, do not provide desired results. The spikes in the graphs of pre-trained models in LFW show unstable validation accuracy during the whole training process, and accuracy is also significantly less than the proposed approach. The reason for getting too many spikes in validation loss can be the large value of the learning rate resolved in the graphs of CPLFW by taking the small value of the learning rate. Therefore, it is suggested to use the LRF curve to identify the optimal learning rate for the model instead of taking random values. If the training loss keeps decreasing while the validation loss increases or remains constant, this is a sign of overfitting. It is evident from Figures 8 and 10 that data overfitting is alleviated by the suggested approach, as shown in Figures 9 and 11. The results in Tables 3 and 5 show that the proposed approach gives better results for VGG19, Resnet50, and DenseNet169; therefore, these three fine-tuned models are considered for designing the ensemble framework (HE-CNN). The proposed modifications in the classification layers and the training process generated SOTA-competent results and improved the recognition accuracy of the pre-trained models in LFW up to approximately 26 and 4% in CPLFW. The proposed ensemble model achieved competent accuracy compared to other existing methods requiring millions of identities to train the network (*i.e.*,

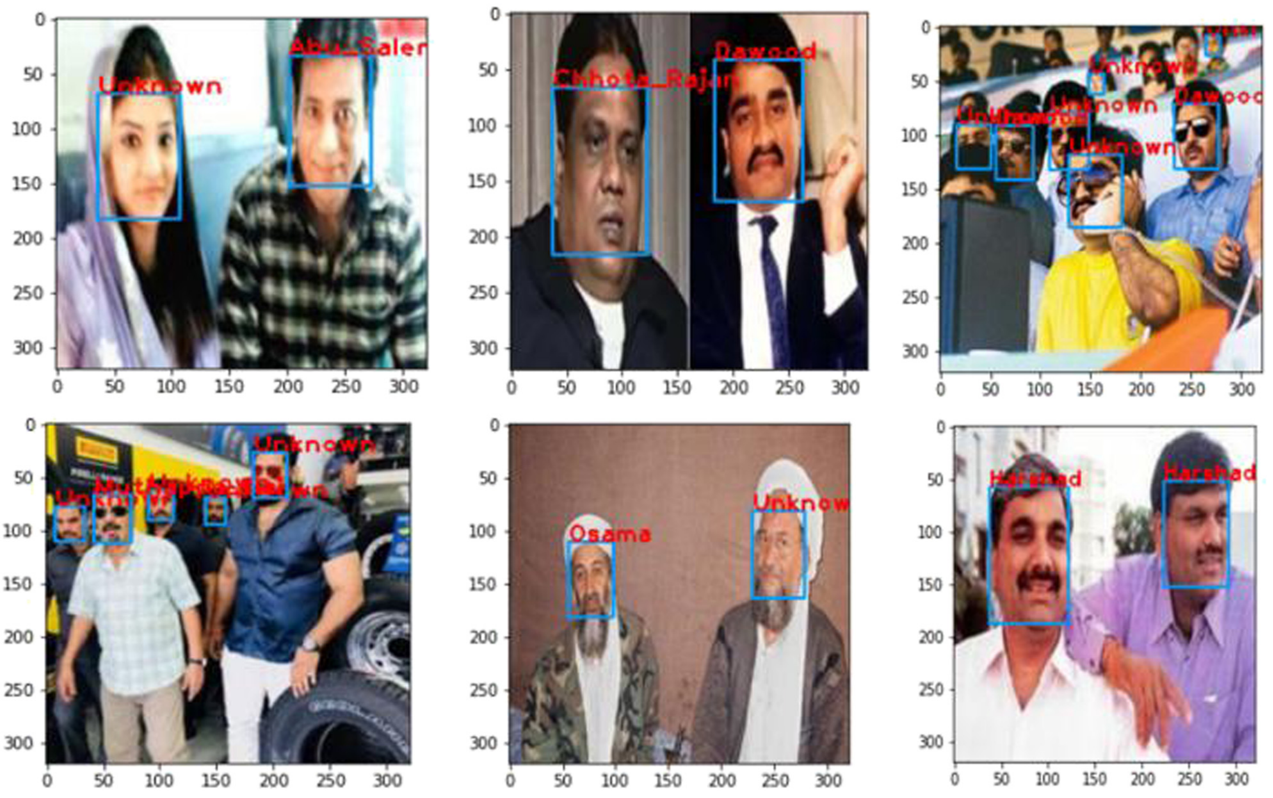

Figure 13: Results of the recognition of criminals in a self-created dataset for testing 50 images.

high GPU memory consumption and computational cost are required for existing methods like ArcFace, FaceNet, *etc*.).

5 Conclusion and future directions

In this work, we perceived that the transfer learning approach is better than other traditional methods. The proposed hybrid architecture (HE-CNN) model for face recognition is designed by performing rigorous experiments. The experimental results of the proposed approach are comparable to SOTA that demand low computational power. Collecting a large number of face images is a difficult task due to people's privacy concerns; therefore, the best solution is provided in the proposed approach using Transfer Learning. Moreover, our model utilized pre-trained models on the ImageNet dataset to extract features, reducing the computational cost and large data requirements. Ensemble transfer learning is implemented, provides better results, and achieves an accuracy of 99.35% in LFW, 91.58% accuracy in CPLFW, and 95% in a self-created dataset. The proposed study can be expanded to include video datasets in experimental evaluation. The self-created dataset can have more image samples in each class by getting new images from the internet or by using other data augmentation techniques such as elastic deformation to simulate the effects of distortions and stretches and the addition of Gaussian noise to help the model learn to recognize objects in noisy environments.

Funding information: No funding was received for this research.

Author contributions: Shahina Anwarul performed the implementation and wrote the methodology and results sections of the manuscript. Tanupriya Choudhury wrote the introduction part and prepared some figures. Susheela Dahiya helped to write the literature review in the introduction section and prepared some figures. Finally, all authors reviewed the complete manuscript.

Conflict of interest: The authors state that no conflicting or other interests affect the findings and discussions presented in this paper.

Data availability statement: The results, data, and figures contained in this manuscript have not been previously published elsewhere, nor are they currently being reviewed by any other publisher for publication.

Third-party material: The authors own all the materials; therefore, no permissions are necessary.

References

[1] Xiao K, Tian Y, Lu Y, Lai Y, Wang X. Quality assessment-based iris and face fusion recognition with dynamic weight. Vis Comput. 2022;38:1631–43.

[2] Min-Allah N, Jan F, Alrashed S. Pupil detection schemes in human eye: a review. Multimed Syst. 2021 Aug;27(4):753–77.

[3] Kortli Y, Jridi M, Al Falou A, Atri M. Face recognition systems: A survey. Sensors. 2020 Jan 7;20(2):342.

[4] Kumar Shukla R, Kumar Tiwari A. Comparative analysis of machine learning based approaches for face detection and recognition. J Inf Technol Manag. 2021 Jan 1;13(1):1–21.

[5] Tan C, Sun F, Kong T, Zhang W, Yang C, Liu C. A survey on deep transfer learning. In: Kůrková V, Manolopoulos Y, Hammer B, Iliadis L, Maglogiannis I, editors. Artificial Neural Networks and Machine Learning–ICANN 2018. 27th International Conference on Artificial Neural Networks; 2018 Oct 4–7; Rhodes, Greece. Springer, 2018. p. 270–9.

[6] Niu S, Liu Y, Wang J, Song H. A decade survey of transfer learning (2010–2020). IEEE Trans Artif Intell. 2020 Oct;1(2):151–66.

[7] Punia SK, Kumar M, Stephan T, Deverajan GG, Patan R. Performance analysis of machine learning algorithms for big data classification: Ml and ai-based algorithms for big data analysis. Int J E-Health Med Commun (IJEHMC). 2021 Jul 1;12(4):60–75.

[8] Vaiyapuri T, Mohanty SN, Sivaram M, Pustokhina IV, Pustokhin DA, Shankar K. Automatic vehicle license plate recognition using optimal deep learning model. Comput Mater Continua. 2021 Jan 1;67(2):1881–97.

[9] Vetriselvi T, Lydia EL, Mohanty SN, Alabdulkreem E, Al-Otaibi S, Al-Rasheed A, et al. Deep learning based license plate number recognition for smart cities. Comput Mater Continua. 2022 Jan 1;70(1):2049–64.

[10] Guo Y, Liu Y, Oerlemans A, Lao S, Wu S, Lew MS. Deep learning for visual understanding: A review. Neurocomputing. 2016 Apr 26;187:27–48.

[11] Sun Y, Wang X, Tang X. Deep learning face representation from predicting 10,000 classes. Proceedings of the IEEE Conference on Computer Vision and Pattern Recognition; 2014 Jun 23–28; Columbus (OH), USA. IEEE, 2014. p. 1891–8.

[12] Parkhi OM, Vedaldi A, Zisserman A. Deep face recognition. BMVC. 2015;1:6.

[13] Huang GB, Mattar M, Berg T, Learned-Miller E. Labeled faces in the wild: A database for studying face recognition in unconstrained environments. Workshop on Faces in 'Real-Life' Images: Detection, Alignment, and Recognition; 2008 Oct; Marseille, France.

[14] Wolf L, Hassner T, Maoz I. Face recognition in unconstrained videos with matched background similarity. CVPR 2011; 2011; Jun 20–25; Colorado Springs (CO), USA. IEEE, 2011. p. 529–34.

[15] Wen Y, Zhang K, Li Z, Qiao Y. A discriminative feature learning approach for deep face recognition. In: Leibe B, Matas J, Sebe N, Welling M, editors. Computer Vision–ECCV 2016: 14th European Conference; 2016 Oct 11–14; Amsterdam, The Netherlands. Springer, 2016. p. 499–515.

[16] Sagi O, Rokach L. Ensemble learning: A survey. Wiley Interdiscip Reviews: Data Min Knowl Discovery. 2018 Jul;8(4):e1249.

[17] Tang J, Su Q, Su B, Fong S, Cao W, Gong X. Parallel ensemble learning of convolutional neural networks and local binary patterns for face recognition. Comput Methods Prog Biomed. 2020 Dec 1;197:105622.

[18] Alhanaee K, Alhammadi M, Almenhali N, Shatnawi M. Face recognition smart attendance system using deep transfer learning. Procedia Comput Sci. 2021 Jan 1;192:4093–102.

[19] Ganaie MA, Hu M, Malik AK, Tanveer M, Suganthan PN. Ensemble deep learning: A review. Eng Appl Artif Intell. 2022 Oct 1;115:105151.

[20] Fayek HM, Cavedon L, Wu HR. Progressive learning: A deep learning framework for continual learning. Neural Netw. 2020 Aug 1;128:345–57.

[21] Barreto S. What is Fine-tuning in Neural Networks?; 2022. https://www.baeldung.com/cs/fine-tuning-nn. Accessed on 24 March 2023.

[22] Lin M, Chen Q, Yan S. Network in network. arXiv preprint. arXiv:1312.4400; 2013 Dec 16.

[23] Basha SS, Dubey SR, Pulabaigari V, Mukherjee S. Impact of fully connected layers on performance of convolutional neural networks for image classification. Neurocomputing. 2020 Feb 22;378:112–9.

[24] Ioffe S, Szegedy C. Batch normalization: Accelerating deep network training by reducing internal covariate shift. In: Bach F, Blei D, editors. International Conference on Machine Learning; 2015 Jul 6–11; Lille, France. ACM, 2015. p. 448–56.

[25] Srivastava N, Hinton G, Krizhevsky A, Sutskever I, Salakhutdinov R. Dropout: a simple way to prevent neural networks from overfitting. J Mach Learn Res. 2014 Jan 1;15(1):1929–58.

[26] Liu W, Anguelov D, Erhan D, Szegedy C, Reed S, Fu CY, et al. SSD: Single Shot MultiBox Detector. In: Leibe B, Matas J, Sebe N, Welling M, editors. Computer Vision–ECCV 2016: 14th European Conference; 2016 Oct 11–14; Amsterdam, The Netherlands. Springer, 2016. p. 21–37.

[27] Zhang K, Zhang Z, Li Z, Qiao Y. Joint face detection and alignment using multitask cascaded convolutional networks. IEEE Signal Process Lett. 2016 Aug 26;23(10):1499–503.

[28] Viola P, Jones MJ. Robust real-time face detection. Int J Comput Vis. 2004 May;57:137–54.

[29] Ahonen T, Hadid A, Pietikainen M. Face description with local binary patterns: Application to face recognition. IEEE Trans Pattern Anal Mach Intell. 2006 Oct 30;28(12):2037–41.

[30] Zheng T, Deng W. Cross-pose LFW: A database for studying cross-pose face recognition in unconstrained environments. Beijing Univ Posts Telecommun Tech Rep. 2018 Feb;5(7):1–6.

[31] He K, Zhang X, Ren S, Sun J. Deep residual learning for image recognition. Proceedings of the IEEE Conference on Computer Vision and Pattern Recognition; 2016 Jun 27-30; Las Vegas (NV), USA. IEEE, 2016. p. 770–8.

[32] Simonyan K, Zisserman A. Very deep convolutional networks for large-scale image recognition. arXiv preprint. arXiv:1409.1556; 2014 Sep 4.

[33] Huang G, Liu Z, Van Der Maaten L, Weinberger KQ. Densely connected convolutional networks. Proceedings of the IEEE Conference on Computer Vision and Pattern Recognition; 2017 Jul 21–26; Honolulu (HI), USA. IEEE, 2017. p. 2261–9.
[34] Russakovsky O, Deng J, Su H, Krause J, Satheesh S, Ma S, et al. Imagenet large scale visual recognition challenge. Int J Comput Vis. 2015 Dec;115:211–52.
[35] Garbin C, Zhu X, Marques O. Dropout vs batch normalization: an empirical study of their impact to deep learning. Multimed Tools Appl. 2020 May;79:12777–815.
[36] Nair V, Hinton GE. Rectified linear units improve restricted Boltzmann machines. In: Fürkranz J, Joachims T, editors. Proceedings of the 27th International Conference on Machine Learning (ICML-10); 2010 Jun 21–24; Haifa, Israel. ACM, 2010. p. 807–14.
[37] He K, Zhang X, Ren S, Sun J. Delving deep into rectifiers: Surpassing human-level performance on imagenet classification. Proceedings of the IEEE International Conference on Computer Vision; 2015 Dec 7–13; Santiago, Chile. IEEE, 2015. p. 1026–34.
[38] Maas AL, Hannun AY, Ng AY. Rectifier nonlinearities improve neural network acoustic models. In: Dasgupta S, McAllester D, editors. Proceedings of the 30th International conference on Machine Learning; 2013 Jun 16–21; Atlanta (GA), USA.
[39] Smith LN. Cyclical learning rates for training neural networks. 2017 IEEE Winter Conference on Applications of Computer Vision (WACV); 2017 Mar 24-31; Santa Rosa (CA), USA. IEEE, 2017. p. 464–72.
[40] Kingma DP, Ba J. Adam: A method for stochastic optimization. arXiv preprint. arXiv:1412.6980; 2014 Dec 22.
[41] Brownlee J. How to Develop a Weighted Average Ensemble With Python; 2021. https://machinelearningmastery.com/weighted-average-ensemble-with-python/ (accessed March 25th, 2023).
[42] Venu SK. An ensemble-based approach by fine-tuning the deep transfer learning models to classify pneumonia from chest X-ray images. arXiv preprint. arXiv:2011.05543; 2020 Nov 11.
[43] Bradski G. The openCV library. Dr Dobb's J Softw Tools Prof Program. 2000;120:122–5.
[44] Branco P, Torgo L, Ribeiro RP. A survey of predictive modeling on imbalanced domains. ACM Comput Surv (CSUR). 2016 Aug 13;49(2):1–50.
[45] Afonja T. Accuracy Paradox; 2017. https://towardsdatascience.com/accuracy-paradox-897a69e2dd9b Accessed on 13 April 2022.
[46] Perez L, Wang J. The effectiveness of data augmentation in image classification using deep learning. arXiv preprint. arXiv:1712.04621; 2017 Dec 13.
[47] Kang K. Comparison of face recognition and detection models: Using different convolution neural networks. Optical Mem Neural Netw. 2019 Apr;28:101–8.
[48] Ben Fredj H, Bouguezzi S, Souani C. Face recognition in unconstrained environment with CNN. Vis Comput. 2021 Feb;37:217–26.
[49] Mishra NK, Singh SK. Regularized Hardmining loss for face recognition. Image Vis Comput. 2022 Jan 1;117:104343.
[50] Liu W, Zhang YM, Li X, Yu Z, Dai B, Zhao T, Song L. Deep hyperspherical learning. Adv Neural Inf Process Syst. 2017;30:1–11.
[51] Cao Q, Shen L, Xie W, Parkhi OM, Zisserman A. VGGFace2: A dataset for recognising faces across pose and age. 2018 13th IEEE International Conference on Automatic Face & Gesture Recognition (FG 2018); 2018 May 15–19; Xi'an, China. IEEE, 2018. p. 67–74.
[52] Liu W, Zhou L, Chen J. Face recognition based on lightweight convolutional neural networks. Information. 2021 Apr 28;12(5):191.